**2026 NDIA MICHIGAN CHAPTER
GROUND VEHICLE SYSTEMS ENGINEERING
AND TECHNOLOGY SYMPOSIUM
POWER & MOBILITY TECHNICAL SESSION
AUGUST 11-13, 2026 - NOVI, MICHIGAN**

METHODS FOR DESIGNING ROTATING COMPONENTS FOR COMPLIANCE TO ISO 1940 BALANCE REQUIREMENTS USING GENERIC 3D CAD SOFTWARE

John Srodawa[1]

[1]US Army DEVCOM GVSC

ABSTRACT

The benefits of specifying balance requirements in terms of an ISO 1940 balance quality grade instead of traditional mass-distance based requirements are discussed along with methods to convert ISO 1940 balance quality grades into permissible imbalance limits at the bearing supports. Methods are developed to determine the expected imbalance values at bearing supports using mass property data from generic 3D CAD software packages without the need for Finite Element Analysis. Practical exercises are presented using these methods to assess a part's compliance to ISO 1940 while still in the conceptual 3D CAD design stage. These practical exercises cover the selection of appropriate geometric tolerances to ensure part balance without the need for post fabrication balancing as well as the design of nonsymmetrical components for ISO 1940 balance compliance.

Citation: J. Srodawa, "Methods for Designing Rotating Components for Compliance to ISO 1940 Balance Requirements Using Generic 3D CAD Software," In *Proceedings of the Ground Vehicle Systems Engineering and Technology Symposium* (GVSETS), NDIA, Novi, MI, Aug. 11-13, 2026.

1. INTRODUCTION

The design of rotating components typically requires consideration for both static and dynamic balance to avoid excessive vibrations during operation. One method of specifying balance requirements for rotating components is to specify the required ISO 1940 balance quality grade on the part drawing. The historical method of specifying balance requirements is to place a maximum allowable imbalance requirement on the drawing in units of oz-in or g-mm. In the author's experience, many engineers within the defense industry, as well as many smaller suppliers to the defense industry, are unfamiliar with the application and interpretation of ISO 1940 balance quality grade requirements.

Furthermore, there are many applications where the cost of balancing a component can easily exceed the fabrication cost of the component. This is especially true for the

DISTRIBUTION STATEMENT A. Approved for public release; distribution unlimited. OPSEC #: 10786

small production volumes encountered with defense articles or during rapid prototyping and R&D activities.

Thus, it would be advantageous to know that a particular component adheres to the needed balance requirements while the part is still in the design phase. This is especially important for nonsymmetrical rotating components. Typically, balancing is the last operation to be performed on a part. Significant schedule delays and cost overruns can be avoided if the engineer is assured that the part will meet balance requirements before the drawings are released for fabrication as opposed to finding out during final balancing that there is insufficient material left for removal to achieve the needed balance requirement. Additionally, it could be possible to determine the required geometric tolerances for the part such that the part achieves the required balance levels without the need to balance the part after manufacturing. This could eliminate the cost and schedule delays associated with balancing the part after fabrication.

This problem can be solved using Finite Element Analysis to predict the imbalance forces imposed by a rotating body. However, this typically requires several iterations between the engineer and the finite element analysist adding cost and schedule to the design effort. Most engineers are very comfortable using common 3D CAD packages to design parts, but many engineers lack the experience or confidence to use FEA tools for routine design. In addition, many smaller non-traditional defense contractors may lack ready access to FEA tools and licenses. For this reason, the author sets out to develop methods to ensure both static and dynamic balance in adherence to ISO 1940 during the design phase using nothing more than common 3D CAD packages and spreadsheet calculations.

2. ISO 1940

2.1. Background

ISO 1940 is an international standard that establishes methods to determine the imbalance requirements needed to achieve both static and dynamic balance of rotating components. For those who are accustomed to seeing the balance of a part specified in units of oz-in or g-mm on a part drawing, ISO 1940 balance quality grades can seem confusing. Some suppliers may be tempted to increase the part quote out of concern of increased risk due to an unfamiliar balance specification.

In reality, ISO 1940 is no different than the historical methods of specifying part balance. The key difference is that ISO 1940 establishes balance quality grades that are application specific while also being independent of both part size and rotational speed. This significantly aids the design engineer in determining what degree of imbalance is acceptable for a particular part, especially for new designs that lack historical corporate knowledge.

For instance, how many oz-in of imbalance are acceptable on a 32 ft diameter four bladed propeller spinning at 105 rpm used to propel a naval vessel? How many g-mm of imbalance are acceptable for an electric motor used to power a drone propeller rotating at 13,000 rpm? Or how many oz-in of imbalance are acceptable on a 2.5 lbm turbocharger spool spinning at 125,000 rpm? Unless the design engineer has corporate knowledge or historical test data to lean on, the answer to these questions would require significant amounts of FEA to determine the acceptable reaction loads at the bearings and support structure in these applications.

However, ISO 1940 makes things significantly easier on the design engineer by specifying balance quality grades for different ranges of applications. For example, ISO 1940 specifies a balance quality grade of G100 for reciprocating engines for cars, trucks, and locomotives. It does not matter if one is designing a 6,500 rpm 1.4 L engine for a compact car, a 2300 rpm 13 L engine for an on-highway truck application, or a 1000 rpm 190 L engine for a locomotive. Using a simple equation, the G100 balance quality grade can be converted to the allowable imbalance considering part mass and rotational speed. Likewise, ISO 1940 specifies balance quality grade G6.3 for aircraft turbines and turbo-chargers. This balance quality grade applies equally to a turbine engine on a Boeing 777, the turbine engine in the Abrams tank, and a turbocharger on a three-cylinder Diesel genset.

2.2. Permissible Residual Unbalance

ISO 1940-1 equation 6 presents a simple means to convert from the ISO 1940 balance quality grade to the permissible residual unbalance[1] (also referred to as allowable imbalance by this author).

$$U_{per} = 1000 * \frac{Balance\ Grade * m}{\omega} \quad (1)$$

where U_{per} is the Permissible Residual Unbalance in g-mm, m is the mass of the rotating system in kg, and ω is the rotational speed in rad/s, which is approximately the speed in rev/min divided by 10.

For example, a 25 kg high speed turbine spool rotating at 50,000 rpm would have an acceptable imbalance requirement of:

$$1000\left(\frac{6.3 * 25}{5000}\right) = 31.5\ gmm$$

Conversely, a 1 kg turbocharger spool rotating at 125,000 rpm would have an acceptable imbalance requirement of:

$$1000\left(\frac{6.3 * 1}{12500}\right) = 0.504\ gmm$$

It should be noted that the Permissible Residual Unbalance is the total allowable imbalance and encompasses both static and dynamic imbalance. The decomposition of this imbalance requirement into static and dynamic limits will be addressed in Section 3.4.

DISCLAIMER: Table 1 of ISO 1940-1 is intended as a guideline for non-critical applications and a starting point for critical applications. Historical knowledge, engineering analysis, and relevant hardware testing must always be considered when determining the appropriate balance quality grade for safety critical applications.

2.3. Static vs Dynamic Imbalance

ISO 1940-1 describes different types of imbalance in Clause 4. In general, static imbalance is an imbalance that acts in a single plane. In other words, the imbalance force is always directed radially outwards from the center of gravity of the rotating body. An example would be spinning a string in the air with a weight tied to the end of the string. This single-plane imbalance is typically called static imbalance since it can be detected on a non-rotating body. For instance, it is possible to balance lawnmower blades and car tires by placing a cone through the center hub and then placing the internal apex of that cone on a pointed fulcrum or needle, as shown in **Figure 1**. If the tire or blade is statically balanced, it will lie perfectly horizontal. If the tire is statically imbalanced, it will lean to one side. The tire or lawnmower blade can then be balanced by adding weights or removing material until it does lie perfectly horizontal. Perfect static balance is achieved when the body's center of gravity is collocated with the body's axis of rotation.

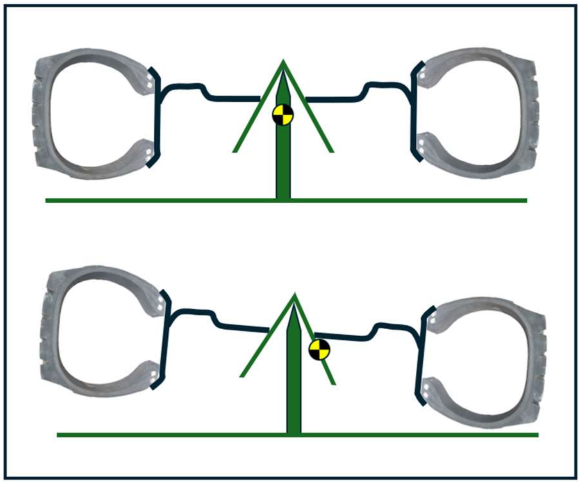

Figure 1: An example of a car tire on a balancing cone showing perfect static balance (top) and static imbalance (bottom)

However, a car tire that has been statically balanced using a balance cone can still cause significant vibrations when driving due to dynamic imbalance. In this situation, the body's center of gravity is located at the bodies center of rotation, but the mass of the body is not symmetrically distributed axially along the length of the body. **Figure 2** shows an example of a rotating body that is statically balanced and dynamically unbalanced. This results in an alternating wobble moment which only occurs when the body is rotating. This imbalance occurs in two planes and in opposite directions resulting in a force couple which generates the wobble moment.

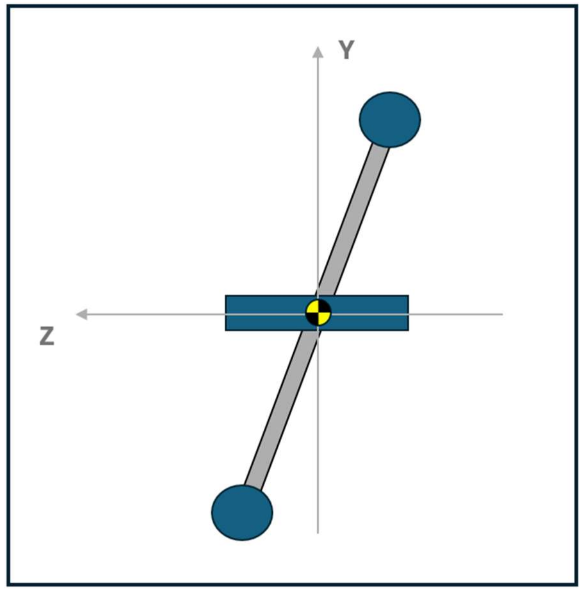

Figure 2: An example of a statically balanced component that is dynamically unbalanced when rotating about the z-axis

3. METHOD DEVELOPMENT

3.1. Static Imbalance

As stated in Section 2.3, static imbalance results when a body's center of gravity is not located on the axis of rotation. As a result, the center of gravity orbits the axis of rotation as the body rotates, as shown in **Figure 3**.

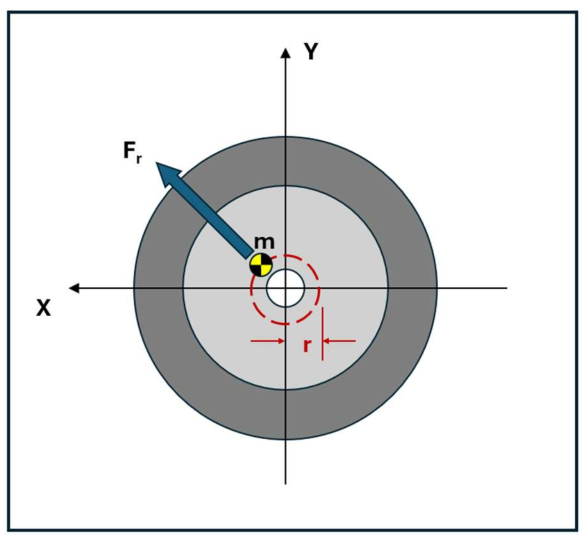

Figure 3: A statically imbalanced body rotating about the z axis

The force generated by the center of gravity orbiting the axis of rotation is simply the mass of the body multiplied by the centripetal acceleration of the center of gravity.

$$F_r = ma_n \tag{2}$$

The centripetal acceleration is a function of the radius of the orbit and the angular velocity of the body.

$$a_n = \frac{v_t^2}{r} = \frac{(r\omega_z)^2}{r} = r\omega_z^2 \tag{3}$$

Thus, the radial force becomes

$$F_r = mr\omega_z^2 \tag{4}$$

The units of the imbalance tolerance are typically given in oz-in or g-mm. This imbalance can be thought of as a weight with a mass m located a distance r from the axis of rotation. Thus, static imbalance is the radial force caused by the orbiting center of gravity divided by the square of the body's angular velocity.

$$U_s = \frac{F_r}{\omega_z^2} = mr \tag{5}$$

Most common 3D CAD packages will provide the mass properties of a part or assembly. The mass properties report provides the mass of the part along with the center of gravity with respect to the specified coordinate system. To determine the static imbalance of the CAD model, simply multiply the mass of the model by the radial distance from the center of gravity to the axis of rotation. Assuming that the selected coordinate system lies on the axis of rotation with the z axis parallel to the axis of rotation, the radial position of the center of gravity can simply be found from the x and y offset to the center of gravity:

$$r = \sqrt{x^2 + y^2} \tag{6}$$

3.2. Dynamic Imbalance

Unfortunately, dynamic imbalance is not so straight forward. Most 3D CAD packages provide a large amount of three-dimensional mass data which includes the inertia tensor and the mass moment of inertias about the principal axes of the model. But there is no single item that clearly shows the imbalance of the model.

To determine how to calculate the model's dynamic imbalance from the model's mass properties, let's first start by defining the moment induced by the dynamic imbalance.

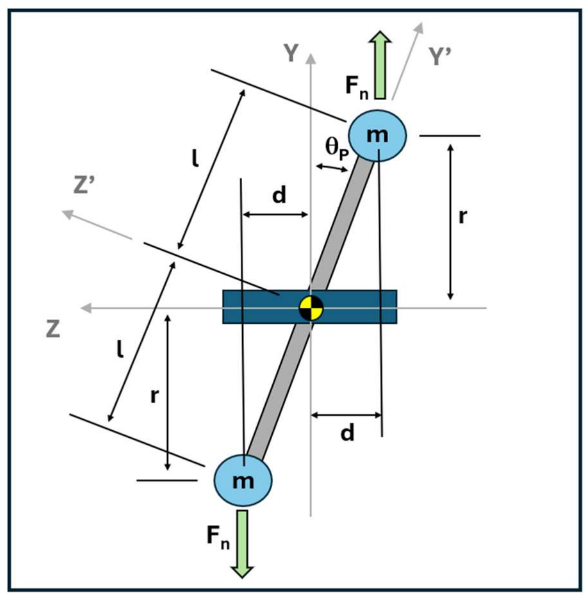

Figure 4: Kinematic description of a dynamically imbalanced body rotating about the z-axis

Figure 4 kinematically describes a dynamically imbalanced body rotating about the z axis. The body consists of two small, dense masses affixed to the ends of a massless stick which is attached to a massless central hub. As the body rotates, each mass generates a radial force, F_n, which acts a distance d from the center of gravity. These two forces, acting together, generate a force couple which generates a moment about the center of gravity. The vector of this moment rotates with the body. As depicted in **Figure 4**, the moment vector lies in the positive x-direction pointing out of the page. When the body has rotated 90°, the moment vector will be pointing in the positive y-direction. Once the body has rotated 180°, the moment vector will lie in the negative x-direction pointing into the page. It should be clear that this moment will thus cause a wobbling force on the body as it rotates, which generates the dynamic imbalance vibrations that one seeks to eliminate.

From **Figure 4**, the radial forces can be defined as

$$F_n = ma_n = mr\omega_z^2 \tag{7}$$

where ω_z represents the angular velocity of the rotating body about the z axis in rad/s. The moment generated by these radial forces about the x axis is

$$M_o = 2F_n d = 2mr\omega_z^2 d \tag{8}$$

Now that the wobble moment has been found, one must consider the effective imbalance at each bearing support in terms of oz-in or g-mm to assess compliance to ISO 1940.

ISO 1940 assesses the allowable dynamic imbalance in terms of the effective point mass and radial position of said point mass at each bearing support which results in the same wobble moment calculated in equation (8). This concept is depicted in **Figure 5**.

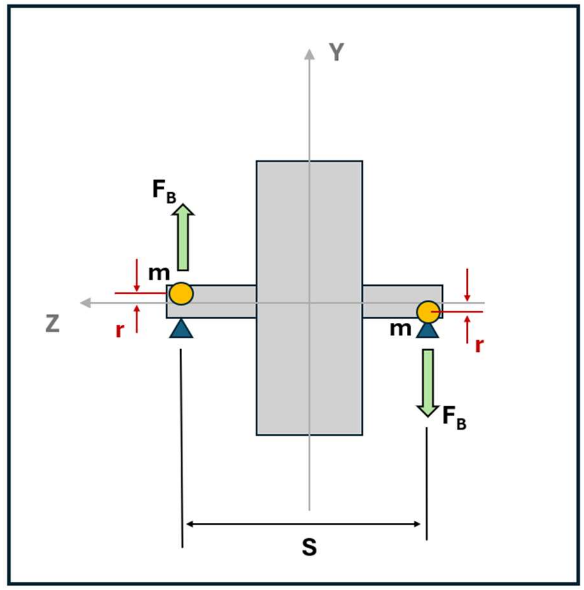

Figure 5: The effective imbalance imposed at each bearing support due to dynamic imbalance on a body rotating about the z-axis

The moment due to the effective imbalance at the bearing supports can be written as

$$M_o = F_B S \tag{9}$$

Where F_B is the reaction force at the bearings and S is the span between bearings. As in equation (4), F_B is a radial force due to a point mass orbiting the axis of rotation.

$$F_B = mr\omega_z^2 \tag{10}$$

Substituting (10) into (9) yields

$$M_o = mr\omega_z^2 S \tag{11}$$

Solving for the dynamic imbalance, mr, results in

$$U_D = mr = \frac{M_o}{\omega_z^2 S} \tag{12}$$

3.3. Motion of a Rigid Body in Three Dimensions

For the general case of a rigid body able to rotate about all three axes, the sum of the moments acting on the body is equal to the time rate of change of the body's three dimensional angular momentum as shown by equation (13) [2].

$$\Sigma \boldsymbol{M}_O = \dot{\boldsymbol{H}}_O = \left(\dot{\boldsymbol{H}}_O\right)_{O_{xyz}} + \boldsymbol{\Omega} \times \boldsymbol{H}_O \quad (13)$$

where H_O is the angular momentum of the body with respect to a fixed coordinate system, $\left(\dot{\boldsymbol{H}}_O\right)_{O_{xyz}}$ is the time rate of change in angular momentum with respect to a coordinate system rotating with the body, and $\boldsymbol{\Omega}$ is the angular velocity of the rotating coordinate system. $\boldsymbol{H}_O$ is found by multiplying the inertia tensor (with respect to the center of gravity) by the body's angular velocity.

$$(\boldsymbol{H}_O)_{O_{xyz}} = \begin{bmatrix} I_{xx} & -I_{xy} & -I_{xz} \\ -I_{yx} & I_{yy} & -I_{yz} \\ -I_{zx} & -I_{zy} & I_{zz} \end{bmatrix} \begin{bmatrix} \omega_x \\ \omega_y \\ \omega_z \end{bmatrix} (14)$$

However, in the specific case of a rotating body supported by two bearings which is only free to rotate about the z axis, equation (14) simplifies to

$$(\boldsymbol{H}_O)_{O_{xyz}} = \begin{bmatrix} -I_{xz}\omega_z \\ -I_{yz}\omega_z \\ I_{zz}\omega_z \end{bmatrix} \quad (15)$$

Taking the first derivative of $(\boldsymbol{H}_O)_{O_{xyz}}$ yields

$$\left(\dot{\boldsymbol{H}}_O\right)_{O_{xyz}} = \begin{bmatrix} -I_{xz}\alpha_z \\ -I_{yz}\alpha_z \\ I_{zz}\alpha_z \end{bmatrix} \quad (16)$$

For a body rotating at a fixed speed, as is typically done on a balancing machine, the angular acceleration about the z axis, α_z, is equal to zero. Thus, $\left(\dot{\boldsymbol{H}}_O\right)_{O_{xyz}}$ is equal to zero.

This just leaves $\boldsymbol{\Omega} \times \boldsymbol{H}_O$. By fixing the rotating coordinate system to the rigid body such that its z axis coincides with the fixed coordinate system's z axis, $\boldsymbol{H}_O$ can be found in a similar manner as was done in equations (14) and (15). Thus

$$\boldsymbol{\Omega} \times \boldsymbol{H}_o = \begin{vmatrix} \hat{\imath} & \hat{\jmath} & \hat{k} \\ 0 & 0 & \omega_z \\ -I_{xz}\omega_z & -I_{yz}\omega_z & I_{zz}\omega_z \end{vmatrix} (17)$$

Substituting (16) and (17) back into (13) results in

$$\Sigma \boldsymbol{M}_O = I_{yz}\omega_z^2\hat{\imath} - I_{xz}\omega_z^2\hat{\jmath} \quad (18)$$

or

$$M_x = I_{yz}\omega_z^2 \quad (19)$$

$$M_y = -I_{xz}\omega_z^2 \quad (20)$$

Now that the moments about the x and y axes have been found, they can be compared to the equation for dynamic imbalance (12). However, in doing so, one should recall that a moment about the x axis is due to forces in the y direction and a moment about the y axis is due to forces in x direction. This results in

$$U_{D_y} = \frac{M_x}{\omega_z^2 S} = \frac{I_{yz}\omega_z^2}{\omega_z^2 S} \quad (21)$$

$$U_{D_x} = \frac{M_y}{\omega_z^2 S} = \frac{-I_{xz}\omega_z^2}{\omega_z^2 S} \quad (22)$$

Thus, the dynamic imbalance is simply the inertia product directly from the inertia tensor divided by the bearing span.

$$U_{D_y} = \frac{I_{yz}}{S} \qquad (23)$$

$$U_{D_x} = \frac{-I_{xz}}{S} \qquad (24)$$

3.4. Simultaneous Consideration of Static and Dynamic Imbalance

It is a rare occurrence when the static and dynamic imbalance occur in the same plane on real parts. ISO 1940-1 contains several figures which demonstrate different possible orientations of the static and dynamic imbalance forces. In some situations, the dynamic imbalance can align with the static imbalance resulting in greater reaction loads on the bearing support. In other cases, the static and dynamic imbalances can partially cancel each other out. Thus, it is important to track both the static and dynamic imbalances in terms x and y components (assuming that the z axis is the axis of rotation).

Consider the general case of a part demonstrating both static and dynamic imbalance, supported by unequally spaced bearings as shown in **Figure 6**.

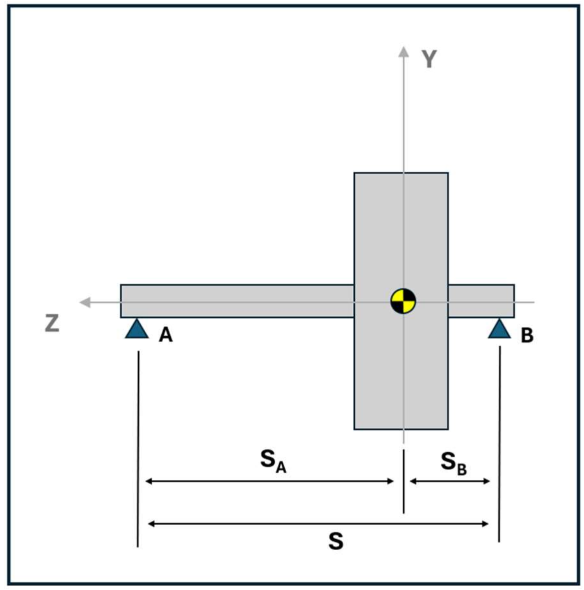

Figure 6: General case for a rotor mounted between support bearings

The total permissible imbalance for this part, U_{per}, is found using Eqn (1) from Section 2.2 of this paper. Per ISO 1940-1, this total permissible imbalance is distributed in proportion to the bearing spacing to determine the maximum permissible imbalance at each bearing support per equations (25) and (26) [1].

$$U_{per_A} = U_{per}\frac{S_B}{S} \qquad (25)$$

$$U_{per_B} = U_{per}\frac{S_A}{S} \qquad (26)$$

These equations are also valid for cantilever mounted rotors as shown in **Figure 7**. It should be noted however, that if the center of mass is located significantly closer to bearing B, that the permissible imbalance on bearing A will become unreasonably small. To avoid this scenario, ISO 1940-1 specifies upper and lower limits on U_{perA} and U_{perB} for both inboard and outboard mounted rotors. Refer to Clause 7.2 of ISO 1940-1 for more information.

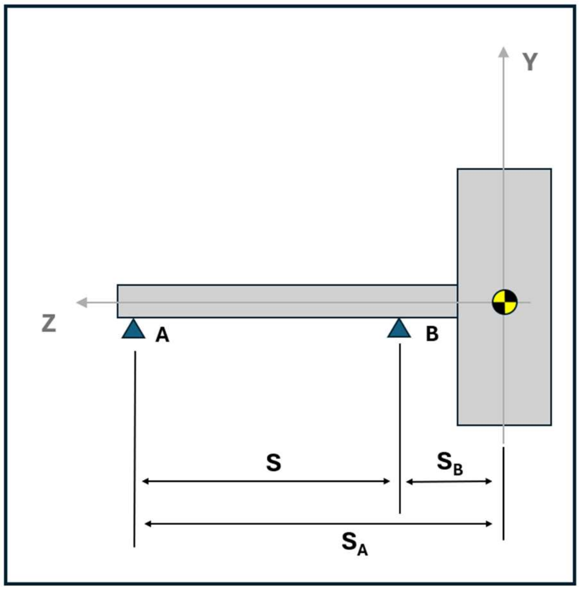

Figure 7: General case for a rotor cantilever mounted outside of the bearing supports

A consideration of the Free Body Diagrams for the scenarios shown in **Figure 6** will reveal that the forces generated by the static imbalance will be proportioned in the same manner as equations (25) and (26). Thus

$$U_{S_{A_X}} = xm\frac{S_B}{S} \qquad (27a)$$

$$U_{S_{B_X}} = xm\frac{S_A}{S} \qquad (28a)$$

$$U_{S_{A_Y}} = ym\frac{S_B}{S} \qquad (29a)$$

$$U_{S_{B_Y}} = ym\frac{S_A}{S} \qquad (30a)$$

where m is the mass of the rotating component, x and y represent the offset between the center of gravity (principal coordinate system) and the reference coordinate system located on the axis of rotation, and U_S is the static imbalance at each bearing support. The sign convention used is consistent with load cells mounted on the positive x and y sides of the rotor shaft which indicate positive values when placed in compression.

For an overhung rotor cantilever mounted outside of the bearing supports per **Figure 7**, a positive x or y center of gravity offset will result in positive reactions at bearing B and negative reactions at bearing A, Thus equations (27a) thru (30a) become

$$U_{S_{A_X}} = -xm\frac{S_B}{S} \qquad (27b)$$

$$U_{S_{B_X}} = xm\frac{S_A}{S} \qquad (28b)$$

$$U_{S_{A_Y}} = -ym\frac{S_B}{S} \qquad (29b)$$

$$U_{S_{B_Y}} = ym\frac{S_A}{S} \qquad (30b)$$

The dynamic imbalance manifests as a moment applied to the center of gravity. By developing the Free Body Diagrams and Equations of Equilibrium for the cases shown in **Figure 6** and **Figure 7Error! Reference source not found.**, one will realize that the reaction forces at the bearing supports due to a moment applied at the center of gravity are independent of the bearing support positions relative to the center of gravity. Rather, the reactions at each bearing due to dynamic imbalance are equal and are only dependent upon the magnitude of the moment and the span between bearings. Thus, equations (23) and (24) are valid for all scenarios involving two bearing supports.

Combining the effects of the static and dynamic imbalances at each bearing support in terms of x and y components results in equations (31a) thru (34a) for rotors that are located in between bearing supports per **Figure 6**.

$$U_{A_X} = xm\frac{S_B}{S} - \frac{I_{xz}}{S} \qquad (31a)$$

$$U_{A_Y} = ym\frac{S_B}{S} - \frac{I_{yz}}{S} \qquad (32a)$$

$$U_{B_X} = xm\frac{S_A}{S} + \frac{I_{xz}}{S} \qquad (33a)$$

$$U_{B_Y} = ym\frac{S_A}{S} + \frac{I_{yz}}{S} \qquad (34a)$$

For overhung rotors cantilever mounted outside of the bearing supports, the combined static and dynamic imbalances in terms of x and y components can be found using equations (31b) thru (34b).

$$U_{A_X} = -xm\frac{S_B}{S} - \frac{I_{xz}}{S} \qquad (31b)$$

$$U_{A_Y} = -ym\frac{S_B}{S} - \frac{I_{yz}}{S} \qquad (32b)$$

$$U_{B_X} = xm\frac{S_A}{S} + \frac{I_{xz}}{S} \qquad (33b)$$

$$U_{B_Y} = ym\frac{S_A}{S} + \frac{I_{yz}}{S} \qquad (34b)$$

The magnitude of the imbalance at each bearing support can be found by combining the X and Y components as follows:

$$U_A = \sqrt{U_{A_X}^2 + U_{A_Y}^2} \qquad (35)$$

$$U_B = \sqrt{U_{B_X}^2 + U_{B_Y}^2} \qquad (36)$$

Now one can confirm that $U_A < U_{perA}$ and $U_B < U_{perB}$. Thus, using equations (31) thru (36) it is possible to determine if a conceptual 3D CAD model adheres to the ISO 1940 imbalance requirements using parameters that are easily obtained from the CAD model mass properties report. Detailed examples of this process will be shown in Section 5.

It is important to stress that the inertia tensor data used in these equations must be taken at the center of gravity, but with respect to the intended coordinate reference frame. This usually comes from the second inertia tensor in the mass properties data report. If one uses inertia tensor data at the reference coordinate system, the inertia products Ixz and Iyz will be artificially large.

One will also find it useful if the intended coordinate reference frame is a coordinate system located on the axis of rotation and in the center of bearing B with the z axis of this coordinate system parallel to the axis of rotation. When this is done, the z offset between the coordinate system and the center of gravity will equal S_B. S_A can then be found from S and S_B.

Tracking the x and y components of the static and dynamic imbalance provides information about the angular position of the imbalance with respect to the part which is critical when modifying the part design to achieve proper balance. The angular position at each bearing support can be found as follows:

$$\gamma_A = \tan^{-1}\left(\frac{U_{A_Y}}{U_{A_X}}\right) \qquad (37)$$

$$\gamma_B = \tan^{-1}\left(\frac{U_{B_Y}}{U_{B_X}}\right) \qquad (38)$$

Care must be taken to observe the signs of the x and y components if one is intending to find the angular position between 0 and 2π (0° and 360°). One may also find it useful to plot the x and y components to visually see the clocking of the imbalances.

4. METHOD VALIDATION

It was desired to develop several test cases where the simplified method developed herein can be validated against traditional methods to assess the method's accuracy.

4.1. Calculating Bearing Reaction Loads from Imbalance Values

This validation involves comparing the reaction loads at the bearing supports predicted by the free body diagrams to the reaction loads calculated from the static and dynamic imbalances determined from the 3D CAD model using equations (31) thru (34). For this comparison to take place, one must convert the predicted imbalance to bearing reaction loads. Referring back to equation (5) and solving for F_r, it can be shown that the radial force due to static imbalance is

$$F_r = U_S \omega_z^2 \tag{39}$$

Determining the reaction loads induced by dynamic imbalance can be found in a similar fashion. Solving equation (9) for F_B results in

$$F_B = \frac{M_o}{S} \tag{40}$$

By rearranging equation (12) it can be shown that

$$\frac{M_o}{S} = U_D \omega_z^2 \tag{41}$$

Thus, the bearing reaction loads due to dynamic imbalance are simply

$$F_B = U_D \omega_z^2 \tag{42}$$

Since the bearing reaction forces due to both static and dynamic imbalance can be found by simply multiplying the respective imbalance by the angular velocity of the body squared, the x and y component of the reaction forces at each bearing can be found from equations (43) thru (46).

$$F_{A_X} = U_{A_X} \omega_B^2 \tag{43}$$

$$F_{A_Y} = U_{A_Y} \omega_B^2 \tag{44}$$

$$F_{B_X} = U_{B_X} \omega_B^2 \tag{45}$$

$$F_{B_Y} = U_{B_Y} \omega_B^2 \tag{46}$$

4.2. Test Case #1

The first test case involves a simple steel component consisting of a 12 mm diameter shaft with a 75 mm diameter rotor 20 mm thick, which rotates at 800 rad/s (7640 rpm). Two lead weights, each measuring 5mm in diameter and 5 mm in length, are attached to the rotor at a radius of 30 mm, as shown in **Figure 8**.

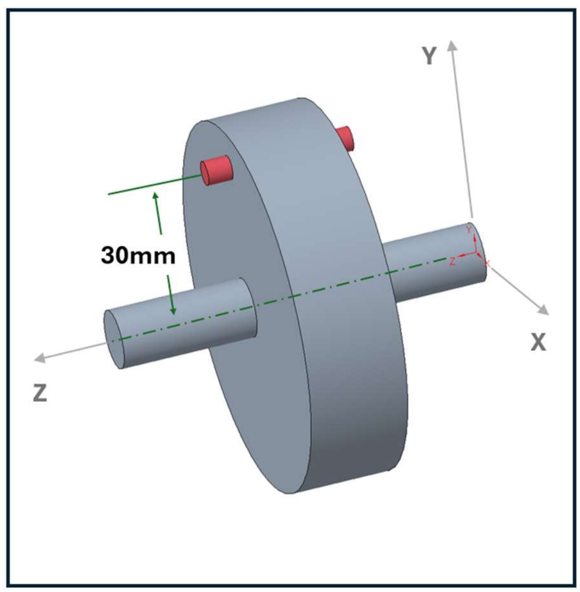

Figure 8: Test case #1 CAD Model

The shaft is 75 mm long with bearings supports at the very end of the shaft. The rotor is centered between the two bearings. Thus

$$\frac{S_A}{S} = \frac{S_B}{S} = 0.5$$

The steel rotor has a mass of 740.3 g and the lead weights have a mass of 1.109 g each. This simple case should be statically imbalanced with perfect dynamic balance. The total static imbalance should have a value of

$$2 * 1.109g * 30mm = 66.54g \cdot mm$$

The values needed to determine the imbalance per Section 3 as depicted in the 3D CAD mass properties report are shown in **Table 1**.

Table 1: Test Case #1 Mass Property Data

Parameter	Value
m [g]	742.5
x [mm]	0
y [mm]	.08965
z [mm]	37.5
I_{xz} [g mm^2]	0
I_{yz} [g mm^2]	0

Solving equations (31a) thru (34a) yields the following imbalances at each bearing.

Table 2: Test Case #1 Calculated Imbalances

Imbalance	Value
U_{Ax} [g mm]	0.00
U_{Ay} [g mm]	33.28
U_{Bx} [g mm]	0.00
U_{By} [g mm]	33.28

The sum of U_{A_y} and U_{B_y} is 66.56 g-mm which compares very closely to the expected static imbalance of 66.54 g-mm.

4.3. Test Case #2

The second test case involves a slight modification to Test Case #1. The steel rotor is identical to Test Case #1, but this time the lead weight closest to bearing B is positioned 30 mm in the negative y direction while the weight closest to bearing A is positioned 30 mm in the positive y direction. This should result in perfect static balance with a measurable dynamic imbalance.

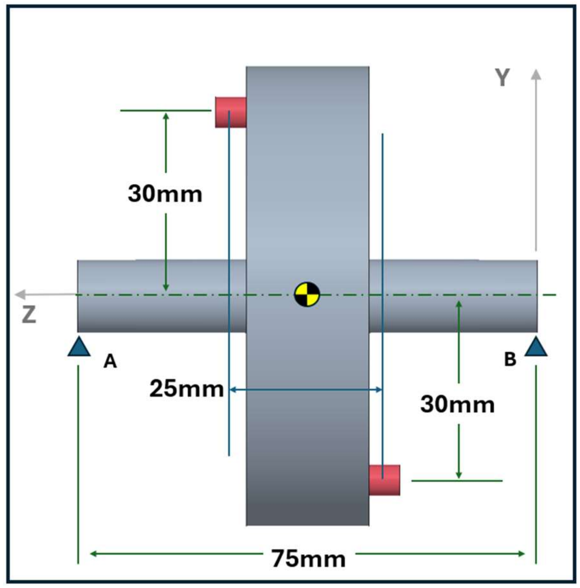

Figure 9: Test Case #2 CAD Model

Substituting (8) into (12) yields

$$U_D = \frac{2mrd}{S} \tag{47}$$

In Test Case #2, the value $2d$ is equal to 25 mm and S is equal to 75 mm. Given the stated values of m and r, the dynamic imbalance should have a value of

$$U_D = (1.109\ g)(30\ mm)\frac{25\ mm}{75\ mm}$$

$$U_D = 11.09\ g \cdot mm$$

The mass properties report from the 3D CAD model provides the necessary values shown in **Table 3**.

Table 3: Test Case #2 Mass Property Data

Parameter	Value
m [g]	742.5
x [mm]	0
y [mm]	0
z [mm]	37.5
I_{xz} [g mm^2]	0
I_{yz} [g mm^2]	-832

Entering these values into equations (31a) thru (34a) results the imbalance values shown in **Table 4**.

Table 4: Test Case #1 Calculated Imbalances

Imbalance	Value
U_{Ax} [g mm]	0.00
U_{Ay} [g mm]	11.09
U_{Bx} [g mm]	0.00
U_{By} [g mm]	-11.09

The imbalance values at the bearings are a perfect match to the expected values. Notice that U_{A_y} and U_{B_y} have opposite signs. This is an indication that this imbalance is due to a dynamic imbalance as opposed to the static imbalance in Test Case #1 which resulted in U_{A_y} and U_{B_y} having the same sign.

4.4. Test Case #3

The third test case assesses a combined static and dynamic imbalance with the rotor offset closer to bearing B. The weight closest to bearing A stays positioned 30mm from the axis of rotation in the positive y direction. The weight closest to bearing B is positioned at a radius of 30 mm, but is clocked 135° in the negative x and negative y directions as shown in **Figure 10**, **Figure 11**, and **Figure 12**.

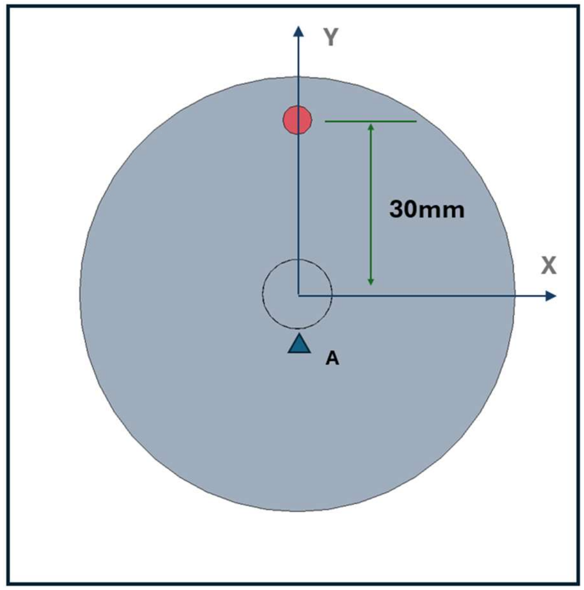

Figure 10: Test Case #3 looking into bearing A

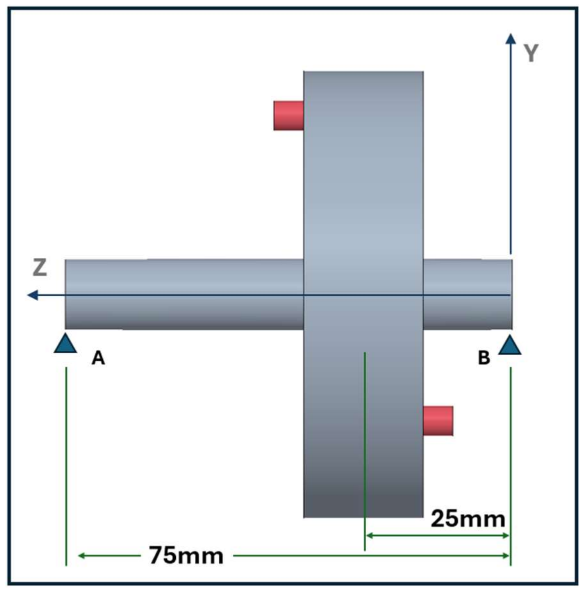

Figure 11: Test Case #3 side view

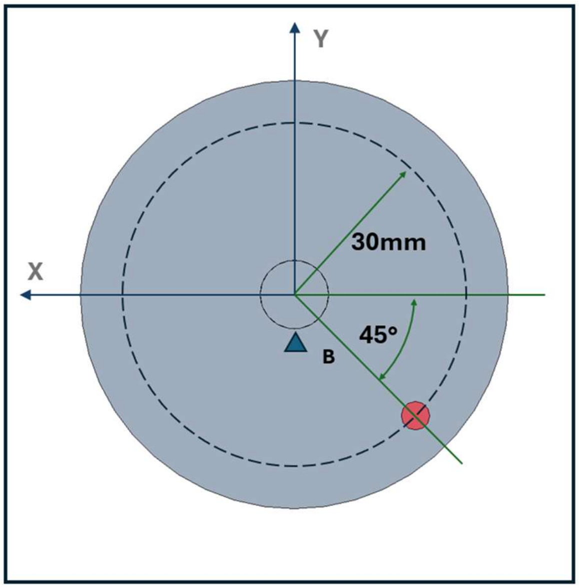

Figure 12: Test Case #3 looking into bearing B

The free body diagram for this test case was examined and the equations of equilibrium were generated for both the xz and yz planes. Solving these equations resulted in the bearing reaction loads shown in **Table 5**.

Table 5: Test Case #3 bearing reaction loads calculated from free body diagrams and equations of equilibrium

Imbalance	Value
F_{Ax} [N]	-2.510
F_{Ay} [N]	8.135
F_{Bx} [N]	-12.54
F_{By} [N]	-1.900

Using equations (43) thru (46), these bearing reaction loads can be converted to imbalance values as shown in **Table 7** assuming an angular velocity of 800 rad/s.

The 3D CAD model mass property data for Test Case #3 is shown in **Table 6**.

Table 6: Test Case #3 Mass Property Data

Parameter	Value
m [g]	742.5
x [mm]	-0.0317
y [mm]	0.0131
z [mm]	26.118
I_{xz} [g mm^2]	-320.5
I_{yz} [g mm^2]	-699.3

The predicted imbalances were found by entering these values into equations (31a) thru (34a). The results are shown in **Table 7** in comparison to the imbalance values found using free body diagrams and equations of equilibrium.

Table 7: Test Case #3 Results Comparison

	From FBD Analysis	From 3D CAD
U_{Ax} [g mm]	-3.922	-3.922
U_{Ay} [g mm]	12.711	12.719
U_{Bx} [g mm]	-19.594	-19.612
U_{By} [g mm]	-2.969	-2.970

4.5. Test Case #4

The fourth test case is a modification of Test Case #3 with the rotor positioned outside of the bearing supports. The mass and location of the lead weights is identical. The total mass increases due to the increased length of the shaft. The 3D CAD model is shown in **Figure 13**.

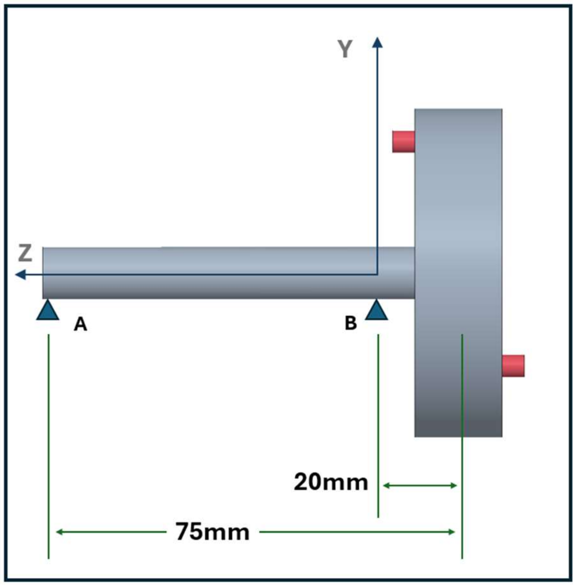

Figure 13: Test Case #4 3D CAD Model

The free body diagrams and equations of equilibrium were established in a manner similar to Test Case #3. The resulting reaction loads at the bearings are shown in **Table 8**.

Table 8: Test Case #4 bearing reaction loads from free body diagrams and equations of equilibrium

Imbalance	Value
F_{Ax} [N]	6.523
F_{Ay} [N]	4.394
F_{Bx} [N]	-21.58
F_{By} [N]	1.842

Using equations (43) thru (46), these reactions loads were converted into imbalance values, which are presented in **Table 10**, assuming an angular velocity of 800 rad/s.

The 3D CAD model mass property data for Test Case #4 is shown in **Table 9**.

Table 9: Test Case #4 Mass Property Data

Parameter	Value
m [g]	769.0
x [mm]	-0.0306
y [mm]	0.0127
z [mm]	-14.863
I_{xz} [g mm^2]	-415.1
I_{yz} [g mm^2]	-660.1

This mass property data was applied to equations (31b) thru (34b) to determine the x and y components of the imbalance at each bearing. These results are shown in **Table 10** compared to the imbalances predicted using free body diagrams and equations of equilibrium.

Table 10: Test Case #4 Results Comparison

	From FBD Analysis	From 3D CAD
U_{Ax} [g mm]	10.192	10.198
U_{Ay} [g mm]	6.866	6.870
U_{Bx} [g mm]	-33.714	-33.731
U_{By} [g mm]	2.878	2.878

4.6. Observations

The correlation between the imbalance predicted by the 3D CAD model property data and the imbalance calculated from detailed free body diagrams and equations of equilibrium is quite good, showing that this simplified method of analyzing component balance using 3D CAD data is robust.

5. PRACTICAL EXCERCISES

In this section, the methods developed in Section 3 are used to predict part imbalance using 3D CAD mass property data while the parts are still in the design phase.

5.1. Exercise #1

There is a desire to design and fabricate a pair of driveshaft adapters for use in testing a heavy combat military vehicle in the GVSC GVPM test cells. The driveshaft adapters are needed to couple the test cell drive shafts to the vehicle final drives. The adapters are 143 lb each and measure 18.5” in diameter by 2.5” thick. One of the adapters is shown in **Figure 14**.

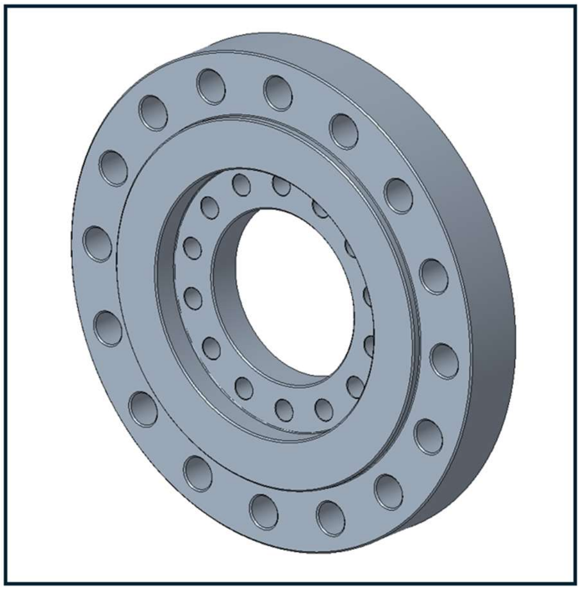

Figure 14: Isometric view of the driveshaft adapter

The quote for fabricating the adapters is \$3500 each. However, the quote for balancing the pair of adapters is an additional \$5500. The high cost associated with balancing is due to the fact that a conjugate adapter is required in order to mount the driveshaft adapters on the balancing machine at the supplier. Since these adapters are machined from solid plate and finished on all surfaces, the mass distribution should be well known. In fact, the greatest variability in mass distribution comes from the drawing tolerances for the design. In order to avoid the additional costs of having the parts balanced, the engineer decides to establish tight enough tolerances to guarantee that the adapters meet balance requirements as machined. However, setting overly tight manufacturing tolerances will also increase the part cost. Thus, there is a need to determine what level of manufacturing tolerance is required in order to meet the balance requirements.

In terms of what balance requirements are needed, one can turn to ISO 1940 for guidance. Based on the general examples found in Table 1 of ISO 1940-1, the engineer determines that a balance quality grade of G16 is appropriate for this application. The maximum speed for these shafts is 800 rpm or 83.78 rad/s. Referring back to equation (1)

$$U_{per} = 1000 \frac{16 * 64.91\, kg}{83.78\, \frac{rad}{s}} = 12{,}400\, g \cdot mm$$

$$12{,}400\, g \cdot mm = 17.22\ oz \cdot in$$

These adapters mount directly to the vehicle final drives. The adapters mount cantilever to the final drive output shaft, so equations (25) and (26) are used to proportion the permissible imbalance to the two bearings. Surveying typical final drives, it is found that S_A = 17”, S_B = 5”, and S = 12” per the definitions set forth in **Figure 7**. Thus the permissible imbalances at each bearing are:

$$U_{per_A} = U_{per} \frac{5}{12} = 0.417 U_{per}$$

$$U_{per_B} = U_{per} \frac{17}{12} = 1.417 U_{per}$$

The relative value of U_{per_B} violates clause 7.2.3 of ISO 1940-1. Thus, U_{per_B} will be limited to $1.3U_{per}$. The final imbalance limits at each bearing are presented in **Table 11**.

Table 11: Permissible imbalance limits at each bearing

	g-mm	oz-in
U_{per_A}	5,167	7.175
U_{per_B}	16,120	22.39

As a starting point, the runout for all non-critical surfaces was set to 0.020" and the positional tolerance for the large bolt holes was set to 0.020". This was modeled by building the 3D CAD model with solids shifted +y by half of the runout, voids shifted -y by half the runout, and the bolt hole pattern shifted -y by half the positional tolerance, with respect to the pilot diameter, as shown in **Figure 15**

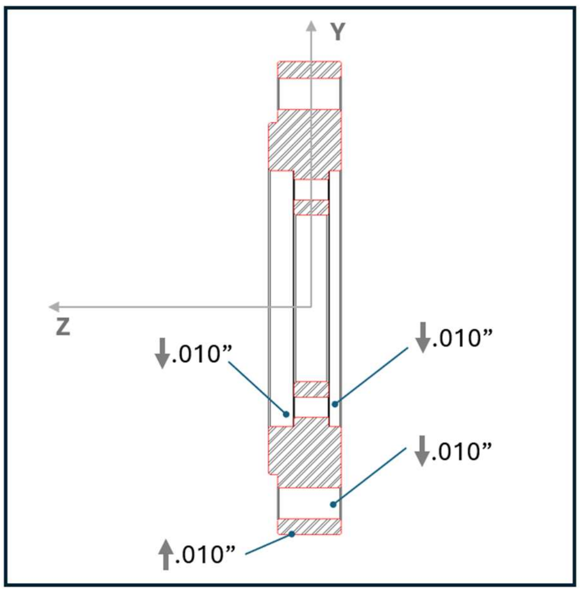

Figure 15: Intentional offsets in model to mimic manufacturing tolerances

The resulting mass property data from the CAD model is shown in **Table 12**.

Table 12: Exercise #1 Mass Property Data

Parameter	Value
m [lbm]	143.1
x [in]	0.0165
y [in]	0.0000
z [in]	1.3110
I_{xz} [lbm in^2]	.01073
I_{yz} [lbm in^2]	0.000

Appling this data to equations (31b) thru (34b) for cantilever mounted rotors results in the imbalance predictions in **Table 13**.

Table 13: Exercise #1 Initial Imbalances

	From 3D CAD
U_{Ax} [oz-in]	-15.76
U_{Ay} [oz-in]	0
U_{Bx} [oz-in]	53.534
U_{By} [oz-in]	0

Using equations (35) and (36), the x and y component values are combined to find the total imbalance magnitude at each bearing to compare to the allowable limits, as shown in **Table 14**.

Table 14: Exercise #1 Initial Results vs Limits

	Predicted	Permissible
U_A [oz-in]	15.76	7.175
U_B [oz-in]	53.53	22.39

Based on these results, the initial tolerances are not tight enough to ensure that the required balance will be achieved without balancing the parts after machining.

It was then decided to reduce the runout tolerance from 0.020" to 0.005" and the hole positional tolerance from 0.020" to 0.010". Both of these changes are achievable at a reasonable cost. The results are shown in **Table 15**.

Table 15: Exercise #1 Final Results vs Limits

	Predicted	Permissible
U_A [oz-in]	4.11	7.175
U_B [oz-in]	13.95	22.39

Thus, using simple methods, it was possible to prove that the finished part will achieve the balance quality needed for this application without the expense of post machining balancing. These same methods could be used on parts that are cast, stamped, welded, or produced using additive manufacturing to avoid the cost of post-production balancing.

5.2. Exercise #2

This exercise deals with the reverse engineering of a damaged part from an expensive piece of equipment that must be replaced. The original part was cast to save money in production. The casting provided excess material to allow for part balancing. The damaged part, shown in **Figure 16**, clearly presents two drillings from the balancing process.

Figure 16: Damaged cast gear subject to reverse engineering

Due to the limited quantities of this part needed to keep the target machinery running, the cost of recasting this part cannot be justified. Additionally, advancements in CNC machining can make machined parts very competitive compared to castings for small to moderate production quantities. However, the part needs to be designed to accommodate ease of machining vs. ease of casting.

The part in **Figure 16** is clearly nonsymmetrical, which was likely done to minimize the mass of metal needed to pour the casting. The first thought was to design the new part to be fully symmetrical as shown in **Figure 17**. This would avoid any balance issues and provide a second set of built-in spare features to accommodate future wear.

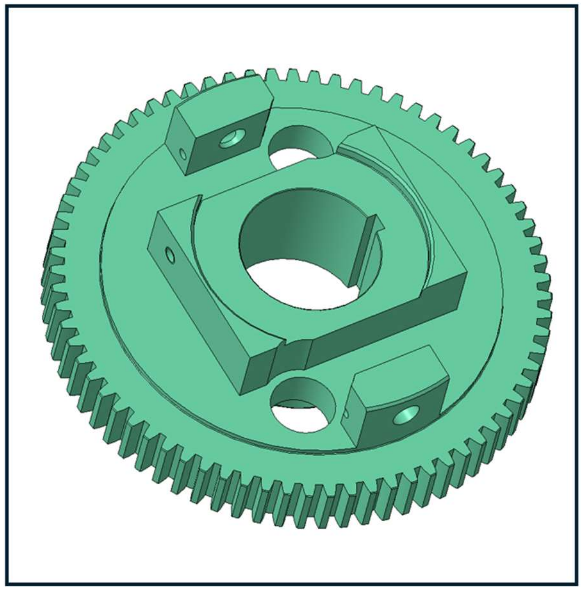

Figure 17: Initial symmetrical part design

Although this results in a perfectly balanced part, this part is just one part in a rotating assembly. The other parts in the assembly are used to selectively engage a drive pin into a hole in a pulley to transfer power in certain operating modes of the machine. For this reason, the full assembly was modeled in CAD to determine the impact of the other components on the overall balance of the assembly. The resulting 3D CAD model is shown in **Figure 18**.

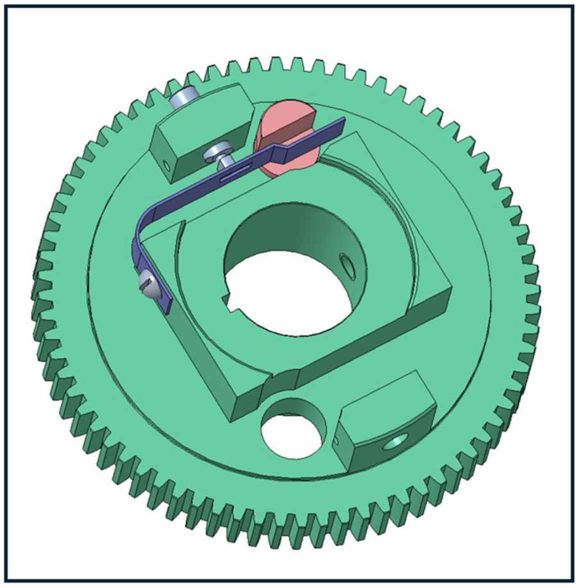

Figure 18: Initial assembly with symmetrical gear

This part is used on a machine tool spindle which rotates at speeds up to 1450 rpm which equates to 151.8 rad/s. Reviewing Table 1 in ISO 1940-1, it was decided that this part should be balanced to a balance quality grade of G6.3. The assembly mass, as shown in **Figure 18**, is 3.639 lbm or 1.65 kg. The permissible imbalance is found using equation (1).

$$U_{per} = 1000\frac{6.3 * 1.65}{151.8} = 68.48\ g \cdot mm$$

For this application, the span between bearings is 3" and the part center of gravity is centered between the bearings. Thus S = 3" and $S_A = S_B = 1.5$". Using equations (25) and (26), the permissible imbalance at each bearing is found to be

$$U_{per_A} = U_{per_B} = 34.24\ g \cdot mm = 0.0475\ oz \cdot in$$

The mass property data for the assembly is shown in **Table 16**.

Table 16: Sym. Assy. Mass Property Data

Parameter	Value
m [lbm]	3.639
x [in]	-.0187
y [in]	-.0544
z [in]	1.500
I_{xz} [lbm in^2]	-.00393
I_{yz} [lbm in^2]	.03229

This mass property data was applied to equations (31a) thru (34a) and equations (35) and (36) to assess the predicted imbalance compared to the permissible limits. The resulting imbalances are shown in **Table 17** and **Table 18**.

Table 17: Exercise #2 Initial Imbalances

	From 3D CAD
U_{Ax} [g-mm]	-376.9
U_{Ay} [g-mm]	-1264.4
U_{Bx} [g-mm]	-407.1
U_{By} [g-mm]	-1016.4

Table 18: Exercise #2 Initial Results vs Limits

	Predicted	Permissible
U_A [g-mm]	1319.4	34.24
U_B [g-mm]	1094.9	34.24

The addition of relatively small parts to the symmetric gear has created an imbalance that far exceeds the permissible values for this balance quality grade. As mentioned at the end of Paragraph 3.4, important information regarding how to correct the balance of a part can be visualized by plotting the x and y components of the imbalance values. This was done and superimposed onto an image of the 3D CAD model in **Figure 19**.

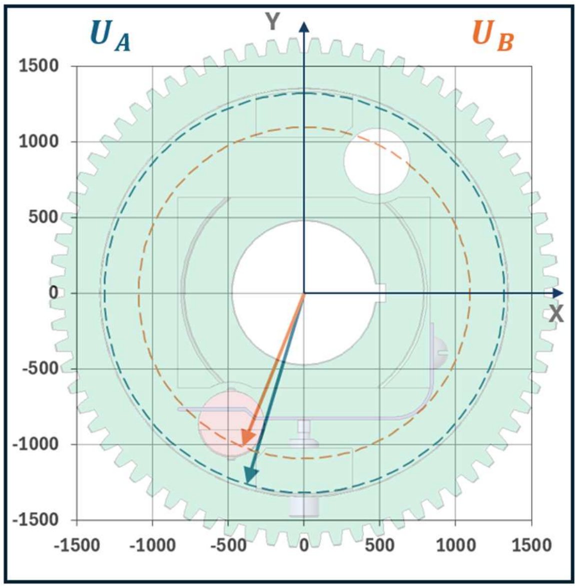

Figure 19: U_A and U_B vectors superimposed on assembly with symmetric gear [g-mm]

As expected, the imbalance is in the direction of the added parts. Note that the two imbalances are not equal and do not point in exactly the same direction. Thus there is a combination of static and dynamic imbalance with static balance dominating the situation. In order to properly balance the assembly, more mass needs to be added to the gear in the upper right corner as viewed in **Figure 19**. In this view, U_A correlates to the front of the part and $U_B$correlates to the back side of the part. Thus, more counterweight needs to be added to the front of the part than the rear of the part. Being that the radial position of the hole in the upper right corner of the part is approximately 40mm from the axis of rotation, approximately 33g needs to be added to the front of the part and 27g needs to be added to the rear of the part. Knowing the density of the material used for the gear, it is then possible to estimate the volume of material that needs to be added to each side of the part.

One option to achieve proper balance would be to add more material than necessary to each side of the part at this approximate location. Then, during balancing, the precise amount of material needed to achieve the necessary balance could be removed. The extra material and the balance drillings could be modeled in 3D CAD to ensure that proper balance is achievable using the mass property data and the methods of Section 3.

One problem with drilling a part to achieve balance is that the part would no longer be balanced if the assembly components are changed in the future. Being that this gear is used on an expensive piece of equipment and spare parts are difficult to obtain, a better option would be to design the part for adjustable balance. Also, for machined parts, it is easier to create localized voids than it is to create localized protrusions. Thus, it was decided to design the part with add on counterweights that can be adjusted to achieve balance. But it is essential to make sure that the design can accommodate mass distribution adjustments that are course enough to handle changes in assembly component mass while still being precise enough to achieve an accurate balance.

The final design is shown in **Figure 20** and **Figure 21**. The updated CAD model includes the shaft, woodruff key, and the set screw that secures the gear to the shaft so that all of these components are included in the imbalance predictions.

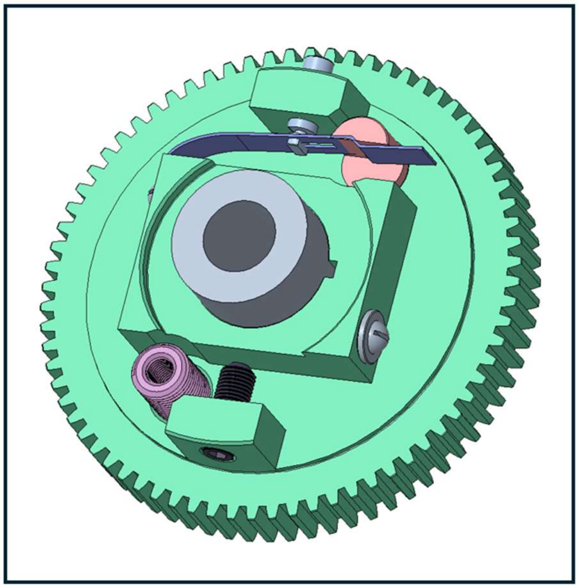

Figure 20: Final design – Front View

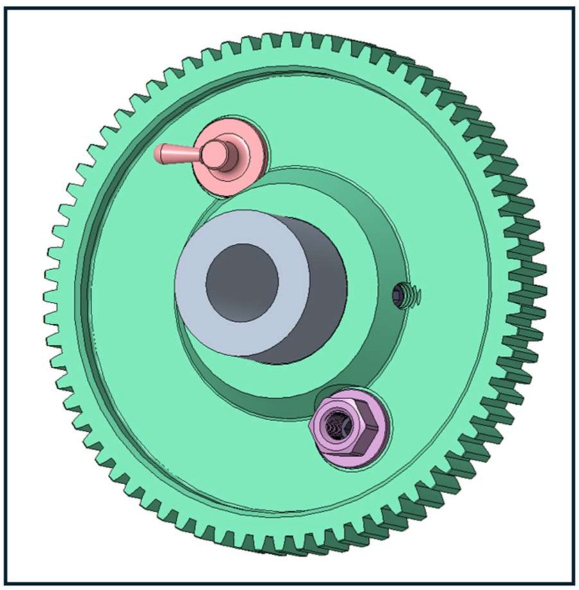

Figure 21: Final Design – Rear View

The design consists of a hollow counterweight slug (purple) that is threaded on both the outside and the inside. This slug is threaded into the gear using nonhardening thread-locker allowing the slug to be removed and replaced with a different length slug in the future if course balance adjustments are needed. The internal threads of the slug accept a 5/16-24 UNF set screw. The set screw length can be varied to fine tune static imbalance while the axial position of the set screw can be adjusted by threading the set screw in or out to fine tune dynamic imbalance. There is also a 3/8-24 UNF set screw placed opposite to the locking pin. The length and position of this set screw can also be adjusted to fine tune static imbalance. A third adjustment is the 10-32 screw and washer located at the lower right side of the center block in **Figure 20**. This screw and washer is meant to counterbalance a portion of the leaf spring and the screw the retains the leaf spring. By varying the diameter and thickness of the washer, the static and dynamic imbalance can be tuned, mostly in the x direction with some y axis influence.

This design was iterated using the methods presented in the paper until an appropriate balance was achieved. The mass properties of the last iteration are presented in **Table 19**. Note that the mass has increased due to the inclusion of the shaft and woodruff key as well as the counterbalance components. With the increase in mass from 3.639 lbm to 4.453 lbm, the allowable imbalance increases from 34.24 g-mm at each bearing to 41.92g-mm.

Table 19: Sym. Assy. Mass Property Data

Parameter	Value
m [lbm]	4.453
x [in]	.00016
y [in]	-.00039
z [in]	1.500
I_{xz} [lbm in^2]	.0029
I_{yz} [lbm in^2]	-.0028

These mass properties were used to update the imbalance predictions which are presented in **Table 20** and **Table 21**. An updated plot of the imbalance vectors overlaid onto the part geometry is shown in **Figure 22**.

Table 20: Exercise #2 Final Imbalances

	From 3D CAD
U_{Ax} [g-mm]	-7.033
U_{Ay} [g-mm]	.0749
U_{Bx} [g-mm]	15.242
U_{By} [g-mm]	-20.758

Table 21: Exercise #2 Final Results vs Limits

	Predicted	Permissible
U_A [oz-in]	7.07	41.92
U_B [oz-in]	25.75	41.92

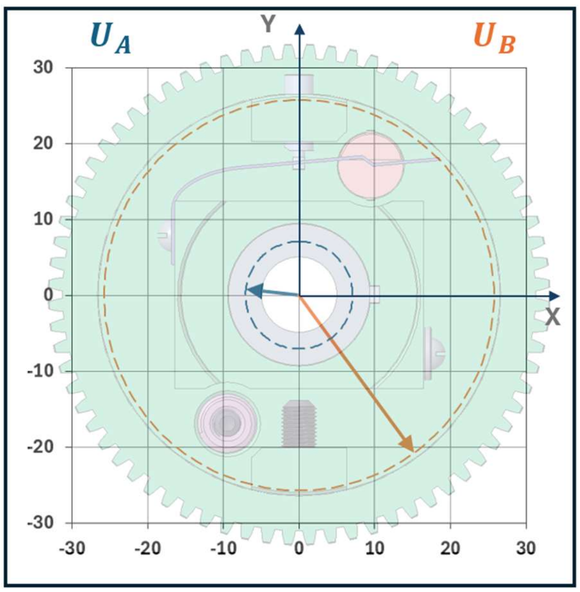

Figure 22: U_A and U_B vectors superimposed on adjustable assembly [g-mm]

The results show that the appropriate balance is achievable with this design. A study of **Figure 22** reveals that the front side of the assembly is well balanced whereas the rear face carries most of the imbalance. The plot implies that more material needs to be added on the back side in the upper left corner or material needs to be removed from the back side in the lower right corner (as viewed in **Figure 22**).

A further study was performed to assess the effectiveness of the adjustments. The first study involved repositioning the 5/16-24 UNF set screw to the most positive z and the most negative z positions possible. These results are show in **Figure 22**. Equations (37) and (38) were used to determine the angular position of the vectors where 0° is along the positive x axis and positive angles are in the CCW direction.

Table 22: Effect of 5/16-24 UNF set screw position on imbalance values

	U_A[g-mm]	U_B [g-mm]
Permissible	41.92	41.92
Baseline	7.07@174°	25.75@306°
Full + Z	26.97@143°	46.85@310°
Full -Z	35.30 @231°	31.46@13°

Next, the effect of adjusting the 3/8-24 UNF setscrew was studied. First, the set screw was screwed in by .125" to the maximum possible positive y position. Then set screws of 7/8" length and 3/4" length were evaluated at the original position (furthest negative y position). The results are shown in **Table 23**.

Table 23: Effect of 3/8-24 UNF set screw position and length on imbalance values

	U_A[g-mm]	U_B [g-mm]
Permissible	41.92	41.92
Baseline	7.07@174°	25.75@306°
1/8" + Y	25.82@106°	18.50@326°
7/8" Long	33.41@102°	16.57@337°
3/4" Long	68.36 @96°	17.62@30°

Lastly, the effects of changing the thickness of the washer located under the 10-32 balance screw were studied. The two cases evaluated were a washer of twice the thickness (.160" vs .080") and the omission of the washer. The results are shown in **Table 24**.

Table 24: Effect 10-32 washer thickness on imbalance values

	U_A[g-mm]	U_B [g-mm]
Permissible	41.92	41.92
.080” THK	7.07@174°	25.75@306°
.160” THK	56.48@336°	52.22@323°
.000” THK	61.29 @171°	25.80@251°

This practical exercise demonstrates that non-symmetrical parts can be designed to accommodate balance requirements to a high degree of precision using simple equations and mass property data that is easily obtained from common 3D CAD software packages. It also demonstrates the ability to use these methods to design assemblies that can be adjusted for balance rather than permanently drilled for balance. This capability could prove useful for precision rotating assemblies in scientific instruments which need to be adjustable or rotating assemblies used in rapid prototyping which may undergo numerous design iterations.

6. IMPLICATIONS FOR DRAWINGS AND THE BALANCING PROCESS

Most legacy drawings and many new drawings specify balance requirements as a single value in units of g-mm or oz-in using a note similar to this:

DYNAMICALLY BALANCE TO WITHIN 0.15 OZ-IN

A general note such as this can lead to confusion later. For example, consider a main cooling fan for a heavy combat military vehicle. The fan impeller weighs 25 lbm and has a maximum operating speed of 6500 rpm. The drawing has the note specified above calling for dynamic balancing to within 0.15 oz-in. There have been several complaints about fan vibrations that are causing premature bearing failures. One of the impellers that was identified as having an issue was traced back to the impeller manufacture by serial number. The fan manufacturer provided an end of line balance test report for that impeller. The report shows that the imbalance at each bearing support was 0.06 oz-in for a total imbalance of 0.12 oz-in which meets the drawing requirements. The engineer investigating the issue sends that impeller to a third-party balancing shop for verification. The third-party test report shows that the imbalance at each bearing support is 0.11 oz-in for a total imbalance of 0.22 oz-in which violates the drawing requirement. Which balance report is correct?

Consider that the impeller has the mass property data shown in **Table 25**.

Table 25: Fan impeller mass property data

Parameter	Value
m [lbm]	25.00
x [in]	.0000
y [in]	.0005
I_{xz} [lbm in^2]	.0030
I_{yz} [lbm in^2]	.0000

One can enter these values into equations (31a) thru (34a) followed by equations (35) and (36) to determine the imbalance at each bearing support. There is only one issue. What is the span between bearings? Upon further investigation it is found that the impeller manufacturer uses a balancing machine with a bearing span of 9” but the third-party balance shop used a balancing machine with a bearing span of 5”. Assuming that the impeller center of gravity is centered between the bearings, the calculations predict that the total imbalance is indeed 0.12 oz-in when using a 9” bearing span and 0.22 oz-in when using a 5” bearing span.

The issue here is that dynamic imbalance generates a moment as opposed to a force, but the balancing machine measures the reaction force at the bearings. So the only way to specify the allowable imbalance on the drawing is the specify the oz-in limit along with a reference bearing span. A conscientious balancing technician may correct the balancing machine reactions to a span equivalent to the mean part thickness, but there is no guarantee that this will be done or that this is what the engineer intended. And this is complicated further by variations in balance machine design especially since some position the part outside the bearings using a cantilever mount while others mount the part between bearings. All of this confusion can be avoided by simply specify that the part be balanced per ISO 1940 with a note similar to:

PART SHALL BE BALANCED IN ACCORDANCE TO ISO 1940 TO A BALANCE QUALITY GRADE OF G6.3 OR LESS

This drawing note will ensure that the part is balanced correctly considering both static and dynamic imbalances while also accounting for the balance machine bearing locations. This type of note also saves time when designing numerous different parts all used in the same application. For example, a supplier making cooling fans for a wide range of air flow levels could apply the same balance quality grade across their entire product line. In this case, one could use the same note on every drawing instead of determining a part specific allowable imbalance value for each part and drawing.

7. CONCLUSION

Although many engineers find ISO 1940 to be an intimidating document, usage of this specification actually reduces engineering effort by allowing streamlined drawing notes which can be common across parts used in similar applications. The decomposition of an ISO 1940 balance quality grade into allowable imbalance values is a relatively easy and straight forward process using the equations in ISO 1940-1 which were reiterated herein. In addition, the simple equations developed in this paper can be used to ensure compliance to ISO 1940 during the design stage using mass property data that any commonly available 3D CAD software package can provide. This method can be used to establish appropriate tolerances on symmetrical parts to avoid post fabrication balancing or to design nonsymmetrical parts to ensure that balance requirements can be met with a minimum amount of material stock held in reserve for balance drillings. These methods ultimately reduce cost, lead times, schedule delays, and part weight.

8. REFERENCES

[1] Mechanical Vibration – Balance Quality Requirements for Rotors in a Constant (Rigid) State – Part 1: Specification and Verification of Balance Tolerances. ISO 1940-1:2003. Geneva, Switzerland : ISO

[2] F. Beer, E. Johnston, "Vector Mechanics for Engineers: Statics and Dynamics, 5th Ed", McGraw-Hill, New York, 1988.

9. CONTACT INFORMATION

John Srodawa
Engine & Transmission Technical Specialist
US Army DEVCOM GVSC
Ground Vehicle Propulsion & Mobility
6501 E. 11 Mile Rd.
Warren, MI 48397
john.p.srodawa.civ@army.mil
571-588-8143

Appendix

One may also question if there is a way to confirm the values of x and y as well as I_{XZ} and I_{YZ} based on the measured values of U_{A_X}, U_{A_Y}, U_{B_X}, and U_{B_Y}. This would allow one to measure CG location and inertia tensor values for a physical rotating object compared to 3D CAD model predictions. Thus, equations (31a) thru (34a) were used to derive equations for x, y, I_{XZ} , and I_{YZ} as functions of U_{A_X}, U_{A_Y}, U_{B_X}, and U_{B_Y}.

From (31a) and (33a), one can find the sum of U_{A_X} and U_{B_X}

$$U_{A_X} + U_{B_X} = xm\frac{S_B}{S} - \frac{I_{XZ}}{S} + xm\frac{S_A}{S} + \frac{I_{XZ}}{S} \tag{48}$$

Equation (48) can be simplified to

$$U_{A_X} + U_{B_X} = xm\left[\frac{S_B + S_A}{S}\right] \tag{49}$$

By observing **Figure 6**, one can see that $S_A + S_B = S$. Thus

$$xm = U_{A_X} + U_{B_X} \tag{50}$$

And

$$x = \frac{U_{A_X} + U_{B_X}}{m} \tag{51}$$

Similarly, equations (32a) and (34a) can be summed to find that

$$ym = U_{A_Y} + U_{B_Y} \tag{52}$$

And

$$y = \frac{U_{A_Y} + U_{B_Y}}{m} \tag{53}$$

From (33a) and (31a), one can find the difference of U_{B_X} and U_{A_X}

$$U_{B_X} - U_{A_X} = xm\left[\frac{S_A - S_B}{S}\right] + \frac{2I_{XZ}}{S} \tag{54}$$

From which one can find that

$$2I_{XZ} = S\left[U_{B_X} - U_{A_X}\right] - xm[S_A - S_B] \tag{55}$$

Substituting (50) into (55) yields

$$2I_{XZ} = U_{B_X}[S - S_A + S_B] - U_{A_X}[S + S_A - S_B] \tag{56}$$

Referring to **Figure 6**, one can see that $S - S_A = S_B$ and that $S - S_B = S_A$. Thus equation (56) reduces to

$$I_{XZ} = S_B U_{B_X} - S_A U_{A_X} \tag{57}$$

Similarly, equations (32a) and (34a) can be used in conjunction with **Figure 6** to solve for I_{YZ}.

$$I_{YZ} = S_B U_{B_Y} - S_A U_{A_Y} \tag{58}$$

Thus, it has been shown that the x and y displacement of the center of gravity from the axis of rotation as well as the inertia tensor values I_{XZ} and I_{YZ} can be found from the measured imbalance values on the balancing machine. Unfortunately, the axial location of the center of gravity must also be known in order to evaluate S_A and S_B. If the load cells on the balancing machine have sufficient dynamic range, the mass of the rotating body as well as the axial location of the center of gravity can be directly measured. Otherwise, each end of the rotating body can be placed on a scale while resting the opposite end on a fixed support with the axis of rotation lying in a horizontal plane to determine the mass and axial location of the center of gravity.

The proceeding derivations are valid for a balancing machine on which the rotating body is located between bearing supports. For balancing machines on which the rotating body is cantilever mounted per **Figure 7**, equations (31b) thru (34b) can be used in conjunction with **Figure 7** to show that

$$x = \frac{U_{A_X} + U_{B_X}}{m} \tag{59}$$

$$y = \frac{U_{A_Y} + U_{B_Y}}{m} \tag{60}$$

$$I_{XZ} = -S_B U_{B_X} - S_A U_{A_X} \tag{61}$$

$$I_{YZ} = -S_B U_{B_Y} - S_A U_{A_Y} \tag{62}$$

If the balancing machine does not directly report the x and y components of the imbalance, they may be found using equations (63) thru (66), taking care to observe sign conventions and quadrants for angles between $\frac{\pi}{2}$ and 2π.

$$U_{A_X} = U_A cos\gamma_A \tag{63}$$

$$U_{A_Y} = U_A sin\gamma_A \tag{64}$$

$$U_{B_X} = U_B cos\gamma_B \tag{65}$$

$$U_{B_Y} = U_B sin\gamma_B \tag{63}$$